

Diagnostics for Ultra-Low Emittance Beams

J.W. Flanagan, KEK

2011.9.7

IPAC11

Outline

- Ultra-low emittance machines
- SR monitors
 - Imaging monitors:
 - Visible light imaging
 - X-ray Pinhole
 - X-ray Fresnel Zone Plate
 - X-ray Refractive Optics
 - Non-imaging monitors:
 - SR interferometer
 - Vertical Polarization Monitor
 - Hybrid:
 - X-ray coded aperture
- OTR/ODR Monitors
 - OTR
 - ODR
- Laser Wire Monitors
 - Laser Wire
 - Shintake Monitor
- Large Angle Beamstrahlung Monitor (Collision Monitor)
- Comments, and possibilities for the future

Some Ultra-Low Emittance Machines

| | Swiss Light Source | ESRF | Diamond | CesrTA (Low Energy Mode) | ATF/ATF2 | SuperB (LER/HER) | Super-KEKB (LER/HER) |
|--|--------------------|-----------|---------|--------------------------|--------------------|------------------|----------------------|
| ε_y (pm-rad) (min) | 3 | <2 (goal) | 1.7 | 10-20 | ~5-30 | ~5 | ~10 |
| σ_y (μm) (at monitor source point) | ~8 | <10 | 6 | ~10 | ~4-6 (37 nm at FF) | ~9 (36 nm at IP) | ~10 (48/62 nm at IP) |
| Beam Energy (GeV) | 2.4 | 6.03 | 3 | 2.085 | 1.3 | 4.18/6.7 | 4/7 |
| | | | | | | | |

- Note: Challenge is really to measure the small (generally vertical) size.

Imaging Monitors

- Diffraction limit on resolution:

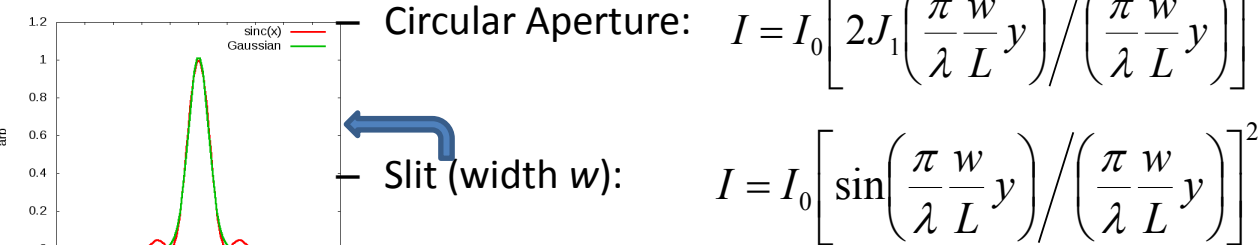
- **Rayleigh criterion:**

- For circular aperture/lens
 - λ = wavelength
 - L = distance from object to aperture/lens
 - » Often close to focal length f for good magnification ($M=f/(f-L)$)
 - w = width (diameter) of aperture
 - δ = separation of two objects where each lies on the first zero of the other's Airy function.

$$\delta = 1.22 \frac{\lambda L}{w}$$

- **Point-spread function:**

- Fit Gaussian to:

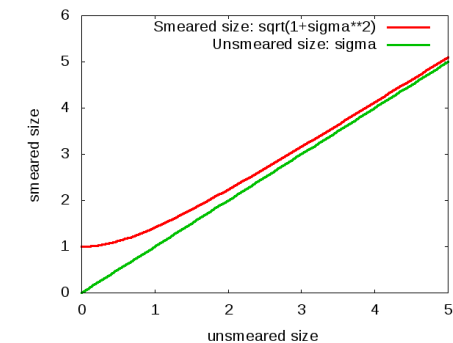


- Treat Gaussian width as smearing function taken in quadrature with beam size:

$$\sigma_{measured} = \sqrt{\sigma_s^2 + \sigma^2}$$

- Both definitions in use out there

$$\left. \sigma_s \approx 0.4 \frac{\lambda L}{w} \right\}$$



SR Imaging

- Intrinsic spread of SR:

$$\sigma_\psi = \begin{cases} 1.07[3\lambda/(4\pi\rho)]^{1/3} & ; \quad \lambda \gg \lambda_c \\ 0.64/\gamma & ; \quad \lambda \approx \lambda_c \\ 0.58[3\lambda\gamma/(4\pi\rho)]^{1/2} & ; \quad \lambda \ll \lambda_c \end{cases}$$

- Plug this into aperture formula

A.J. Kim, AIP Conf. Proc. 184 (1989)

- Setting $w/L = 2\sigma_\psi$
 - → Unless free to vary E or ρ , the minimum theoretical resolution becomes purely dependent on λ .

- For short-wavelength visible light ($\lambda = 400 \text{ nm}$):

- $E = 3 \text{ GeV}, \rho = 30 \text{ m} \Rightarrow \sigma_s = \sim 50 \mu\text{m}$
 - Or, to get $\sigma_s = \sim 10 \mu\text{m}$ at 3 GeV $\Rightarrow \rho = 25 \text{ cm} (!)$

- So, attention quickly turns to x-rays:

- $E = 3 \text{ GeV}, \rho = 30 \text{ m}, \lambda = 1 \text{ nm (1.24 keV)} \Rightarrow \sigma_s = \sim 2 \mu\text{m}$
 - $E = 3 \text{ GeV}, \rho = 30 \text{ m}, \lambda = 0.1 \text{ nm (12.4 keV)} \Rightarrow \sigma_s = \sim 0.2 \mu\text{m}$

X-ray Imaging: Pinhole Optics

- For pinhole optics, the resolution is a balance between diffraction limit (hole too small) and geometric blurring (hole too large).
- Analytical estimate:
 - Geometric blurring:
 - Diffraction limit:
 - →Optimum aperture:
 - →Point-spread:

$$\sigma_A = A_{\text{ph}} \frac{D + d}{d} \frac{1}{\sqrt{12}}$$

$$\sigma_{\text{diff}} = 0.61 \lambda D / A_{\text{ph}}$$

$$A_{\text{ph}}^{\text{opt}} = \sqrt{\frac{\sqrt{3.66} \lambda d D}{D + d}}$$

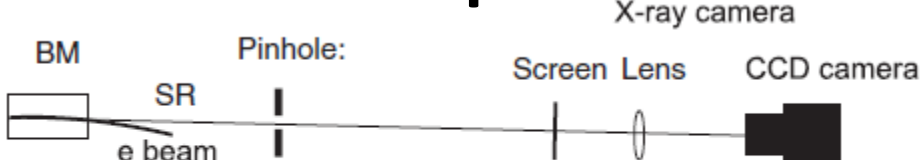
$$\sigma_{\text{psf}}^{\text{min}} = 0.6 \sqrt{\frac{\lambda D(D + d)}{d}}$$

Notes:
d=source->pinhole
D=pinhole->screen
Apertures are half-widths
Sigmas expressed at **detector screen**
(Take out magnification to get at beam)

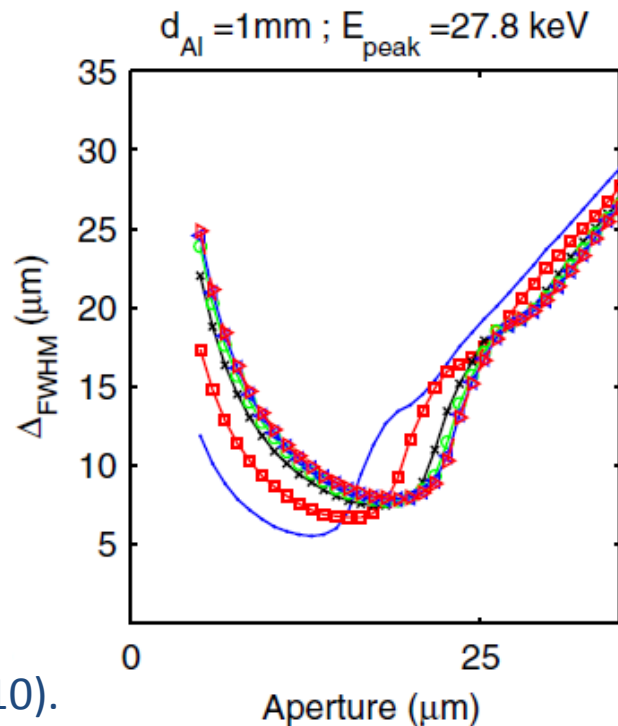
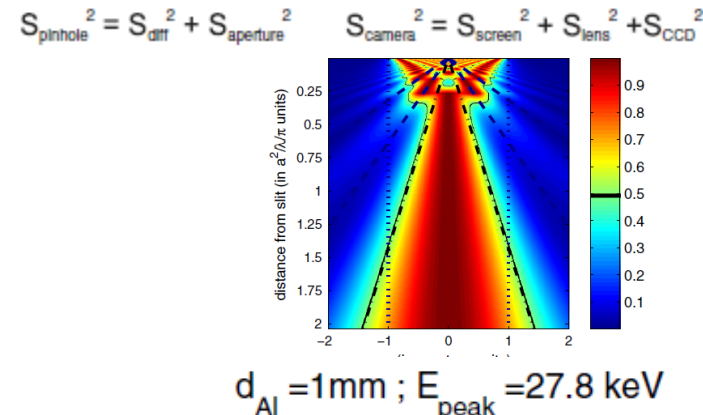
F. Ewald, et al., Proc. DIPAC2011 MOPD61 (2011).

P. Elleaume, et al., J. Synchrotron Rad. 2 (1995) 209.

X-ray Imaging: Pinhole Optics



- More detailed optimization at DIAMOND:
 - Calculate Fresnel diffraction pattern due to pinhole for a point source illuminating the pinhole evenly, over spectrum seen by detector
 - Fit gaussian to resulting PSF at detector screen
 - Add in detector resolution in quadrature
- Results:
 - σ_s (at source) of $6.4 \mu\text{m}$ achieved
 - $\sim 6 \mu\text{m}$ beam size measured
 - σ_s of $2.9 \mu\text{m}$ possible with new aperture and detector screen
 - CdWO₄ screen resolution dominates, contributing $2.6 \mu\text{m}$ (pinhole contributes $1.33 \mu\text{m}$).
 - Note: with 1 mm Al window and 9 m air path, x-ray spectrum peaks at 28 keV.

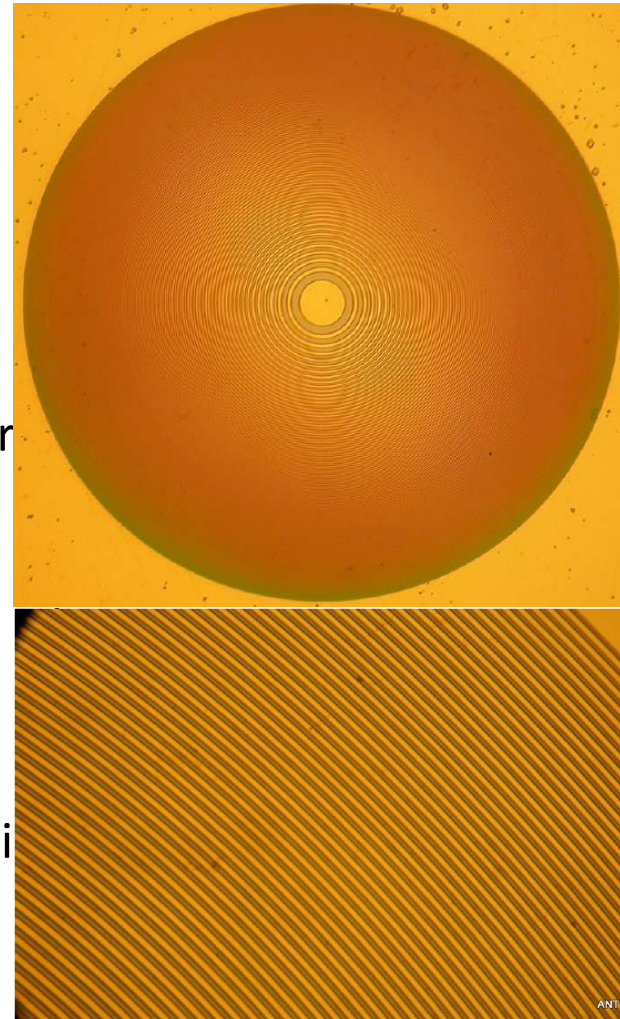


X-ray Imaging: Fresnel Zone Plate

- Fresnel zone plate behaves like a lens
 - Needs monochromator to avoid chromatic aberration.
- Consists of concentric alternating bands of open and filled regions, with radius of boundary n given by:

$$r_n \approx \sqrt{nf\lambda}$$

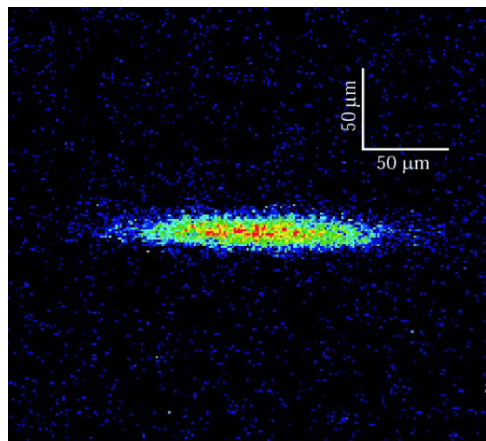
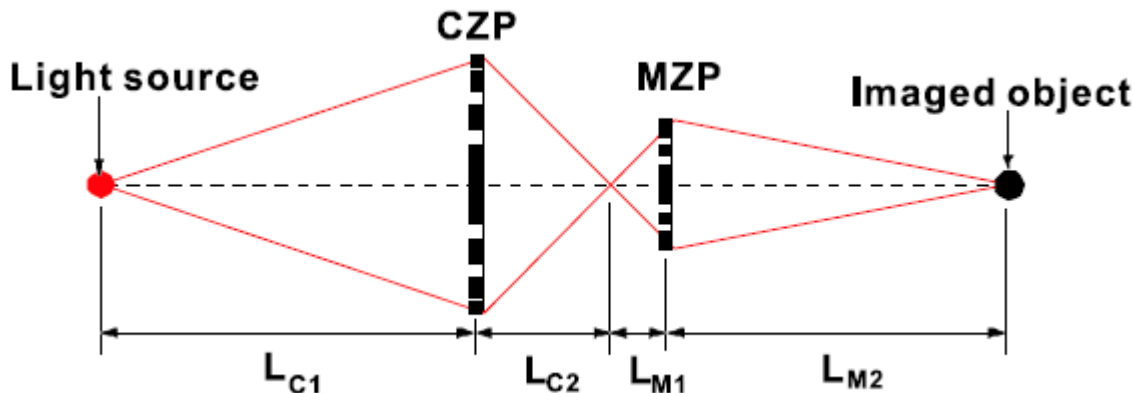
- Constructive interference produces focal point at center (plus higher orders).
- The equivalent of the Rayleigh criterion for a Fresnel zone plate is: $\delta = 1.22\Delta r_n$
 - Δr_n is the width of the outermost zone.
- Currently zone plates with outer zone widths of 45 nm, with mask thickness of 900 nm (depth/width aspect ratio = 20) have been reported used up to 8 keV.
[Y.S. Chu et al., Appl. Phys. Lett. 92, 103119 \(2008\).](#)
- Consequently, the practical resolution limit is not the lens fabrication, but the SR divergence angle at a few keV.



Applied NanoTools

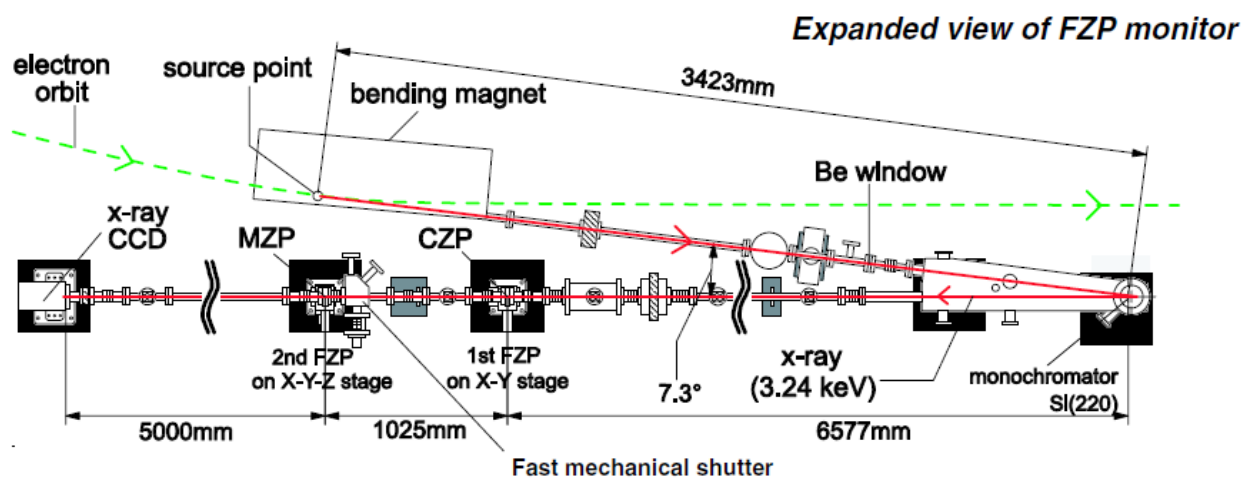
X-ray Imaging: Fresnel Zone Plate

Setup at ATF



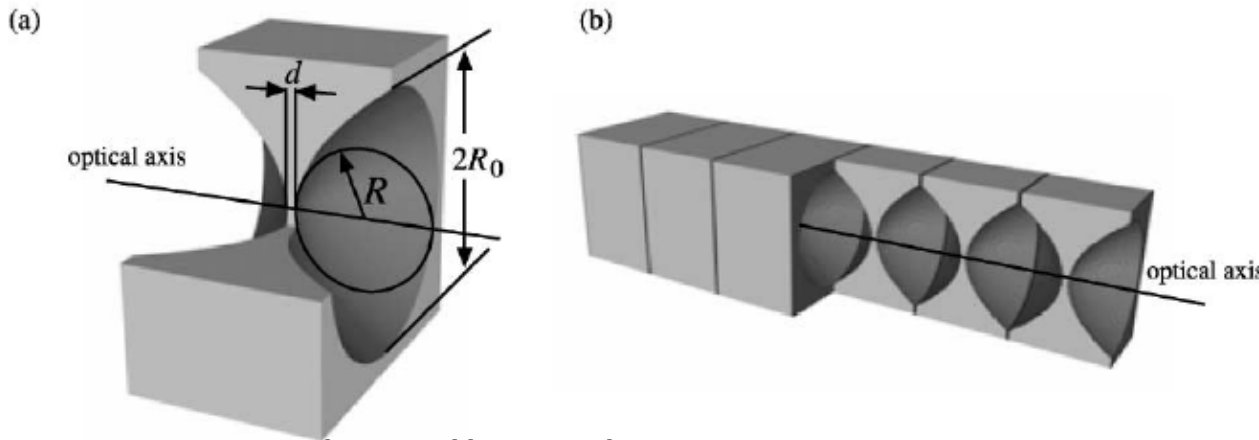
- 2-D imaging
 - $\sigma_y = 6 \mu\text{m}$
 - $\sigma_x = 50 \mu\text{m}$

- Double lens telescope:
 - Resolution: $< 1 \mu\text{m}$ @ 3.24 keV
 - Magnification = 20
 - Detector: x-ray CCD, 24 $\mu\text{m} \times 24 \mu\text{m}$ pixels
 - 20 ms mechanical shutter



H. Sakai, et al., PRST-AB 10 042801 (2007).

X-ray Imaging: Refractive Optics



- Aluminum or beryllium lens
 - $n < 1$ ($\sim 1-1e-6$ at 20 keV for Al)
 - Lens must be convex, not concave, to focus.
 - Weak focusing means stack of lenses needed to achieve a practical focal length.
 - Surface does not have to be as smooth as grazing-incidence mirror would be.
- Rotational parabolic lens surfaces
 - No spherical aberration

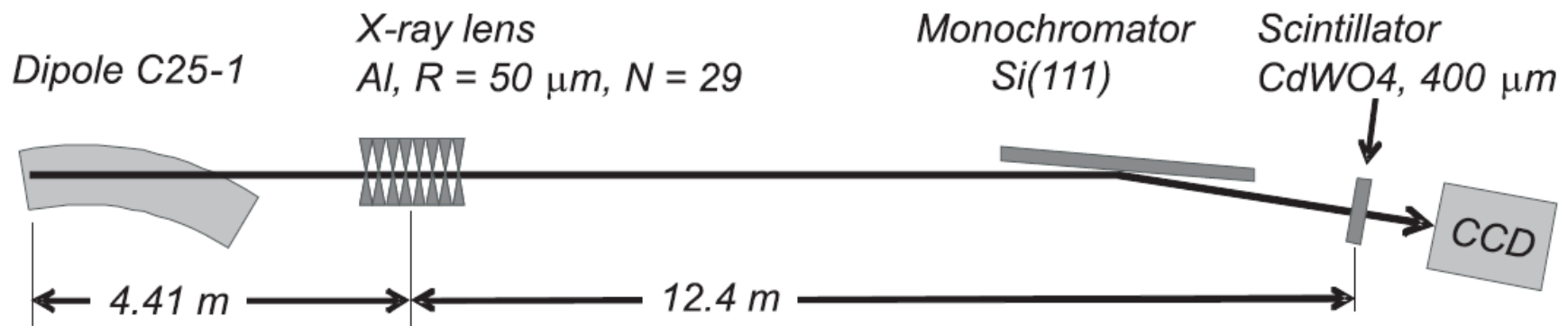
$$n = 1 - \delta + i\beta$$

$$f = R/2N\delta(E)$$

B. Lengeler *et al.*, “Parabolic refractive X-ray lenses: a breakthrough in X-ray optics ,” NIM A 467-468 p. 944-950 (2001).

X-ray Imaging: Refractive Optics

Setup at ESRF



- Aperture becomes limited by absorption in lens material as it becomes thicker away from the axis.
 - Aluminum lens with radius of curvature of 50 μm has effective aperture A_{eff} of $\sim 300 \mu\text{m}$.
- Diffraction limit $1.22 \lambda f / A_{\text{eff}} = \sim 0.5 \mu\text{m}$ at 35 keV.
 - Note: $f=3.25 \text{ m}$, magnification $(f/(f-L)) = 2.8$
 - → Resolution of detector becomes limiting factor if not $< 1.4 \mu\text{m}$.
 - In any case minimum expected beam size is $\sim 7 \mu\text{m}$ (at 1 pm-rad) or $\sim 20 \mu\text{m}$ at detector (CdWO₄ scintillator).

SR Non-imaging: SR Interferometer

- **Variation on Michelson Stellar Interferometer:**
 - Measure smearing of two-slit interference pattern caused by finite source extent.
 - Van Cittert-Zernike theorem: complex degree of spatial coherence γ is Fourier transform of source intensity profile:

$$\gamma(v) = \int f(y) \cdot \text{Exp}(-i2\pi v \cdot y) dy$$

T. Mitsuhashi, Proc. Joint US-CERN-Russia School on Particle Accelerators, Beam Measurement, World Scientific, Singapore, 1998, 399.

- For a Gaussian beam, the beam size as a function of measured visibility (peak-valley ratio) γ is:

$$\sigma = \frac{\lambda}{\pi} \frac{L}{D} \sqrt{\frac{1}{2} \ln\left(\frac{1}{\gamma}\right)}$$

- Generally use horizontal polarization component of SR (higher intensity than vertical)

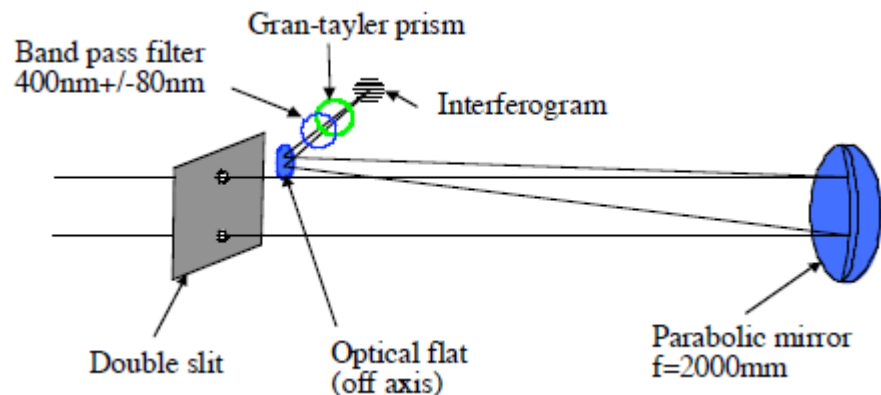
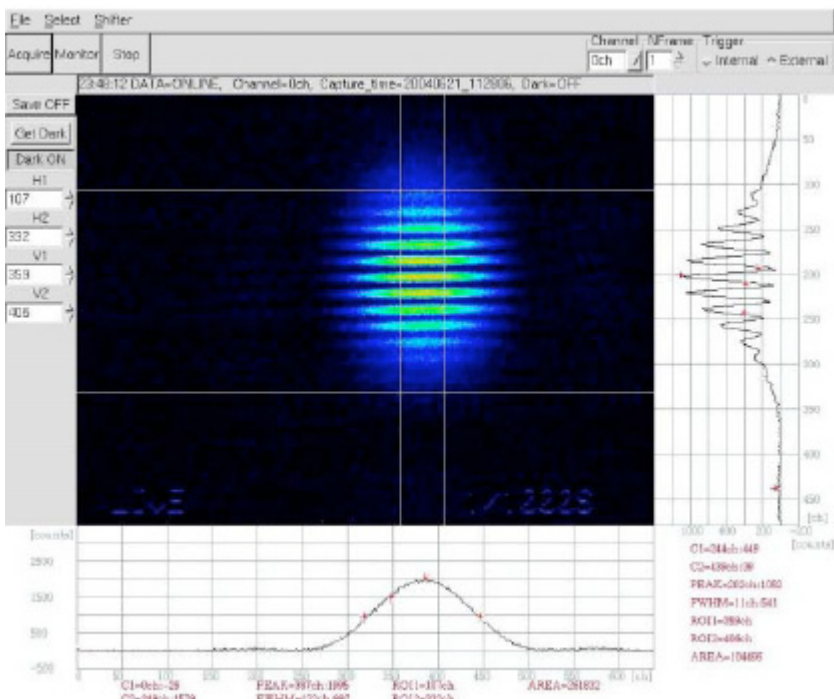
- **Resolution limit determined by:**

- How well one can measure visibilities that are asymptotically approaching 1.
- How wide the slit separation can be made.
- If $\gamma_{\max} = 0.9$, and $D/L = 4 \sigma_\psi$, then get about 1 order of magnitude improvement on imaging resolution.

Cf. Imaging resolution: $\sigma_s \approx 0.4 \frac{\lambda L}{w}$

SR Non-imaging: SR Interferometer

Beam size measurements less than 5 microns demonstrated at ATF, using reflective optics to avoid chromatic aberration of objective lens over filter bandpass:



SR Non-imaging: Vertical Polarization Monitor

- Essentially an interferometer, but using the vertical polarization component.
 - Weaker than horizontal polarization component, BUT has natural zero at center, due to phase reversal, at all wavelengths.
 - Can in principle use a wider bandwidth
 - Double-lobed structure of vertical component provides a “natural” double-slit interferometer even with no limiting aperture.
- In case of no limiting aperture, the vertical E-field at the detector (sqrt of intensity) is:

$$E_\pi(x, y) = E_{\pi 0} \operatorname{sinc}\left(\frac{2\pi x_c}{\lambda p'}x\right) \times \int_0^{+\infty} (1 + \xi^2)^{1/2} \xi K_{1/3}\left(\frac{1}{2} \frac{\lambda_c}{\lambda} (1 + \xi^2)^{3/2}\right) \sin\left(\frac{2\pi p}{\lambda p'} y \xi\right) d\xi$$

A. Hofmann, F. Meot, Nucl. Instr. and Meth. A 203 (1982) 483.

- In fact, SLS calculates point-response functions for different origin positions, using Kirchhoff integral over aperture (which includes cold finger at center of beam).

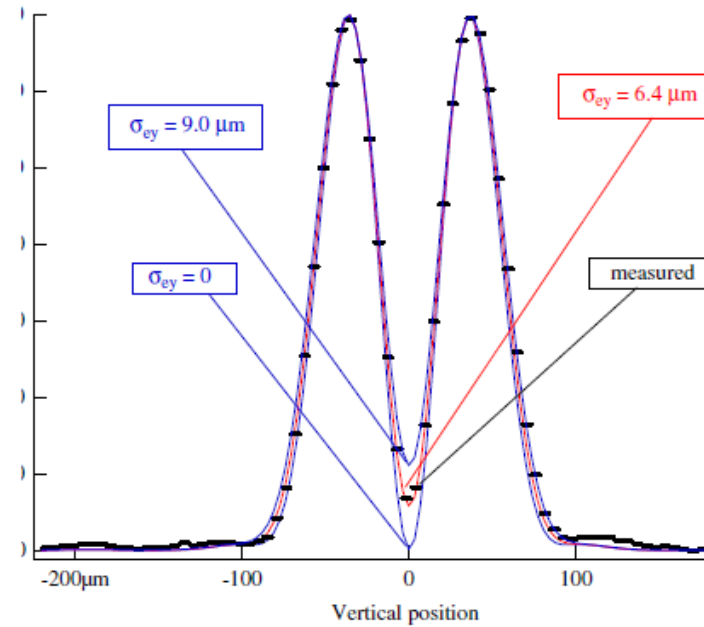
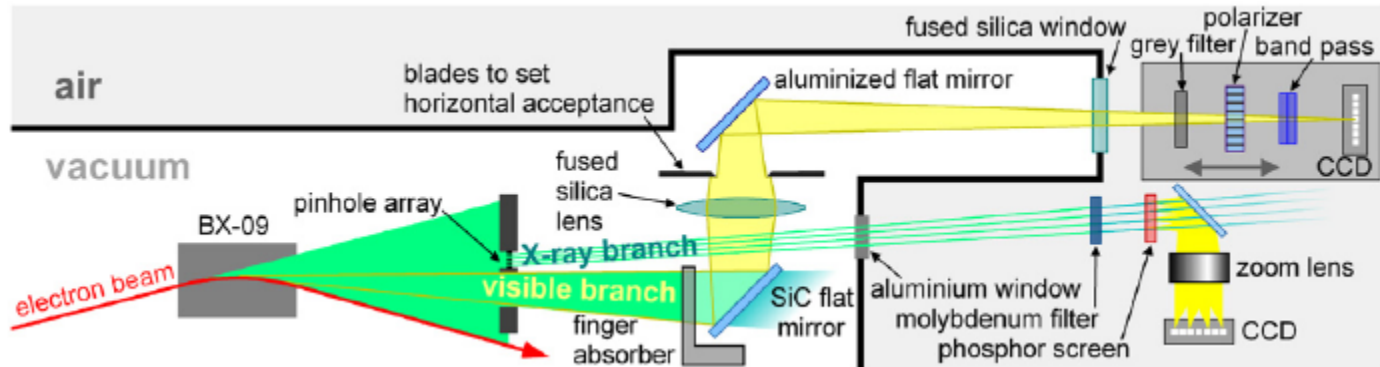


Fig. 8. Measured (marks) and predicted (three solid lines) vertical image profiles. $\lambda = 364$ nm; acceptance angles $3.9 \text{ mrad}_H/9.0 \text{ mrad}_V$. Machine conditions: 400 mA in top-up operation; tuned skew quads.

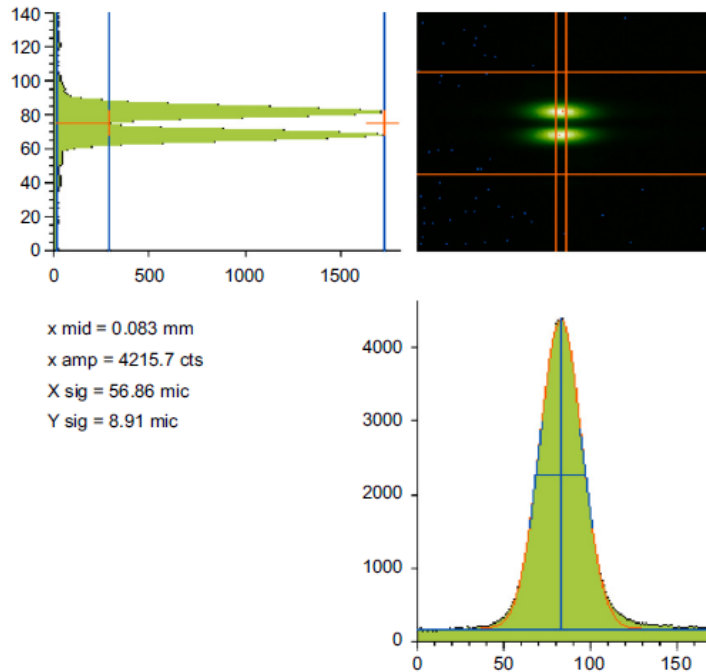
A. Andersson *et al.*, Nuclear Instruments and Methods in Physics Research A 591 (2008) 437–446

SR Non-imaging: Vertical Polarization Monitor

A . Andersson *et al.*,
Nuclear
Instruments and
Methods in Physics
Research A 591
(2008) 437–446



- Resolution limit in principle similar to that of SR interferometer
- Beam size measurements of ~6 microns demonstrated at Swiss Light Source.



Hybrid: X-ray Coded Aperture

- Another (x-ray) astronomy technique: multiple pinholes in pseudo-random pattern
- Reconstruction requires simulation of full diffraction and absorption characteristics of mask, plus detector response, over spectrum.
 - No monochromator
- Pseudo-random pattern gives relatively flat spatial frequency response. (Good for reconstruction).
- Large aperture enables single-shot measurements at resolutions somewhat better than a pinhole camera.
 - Some peak-valley ratios available.

Source distribution: $\begin{bmatrix} A_\sigma \\ A_\pi \end{bmatrix} = \frac{\sqrt{3}}{2\pi} \gamma \frac{\omega}{\omega_c} (1 + X^2) (-i) \begin{bmatrix} K_{2/3}(\eta) \\ \frac{iX}{\sqrt{1+X^2}} K_{1/3}(\eta) \end{bmatrix},$

where

$$X = \gamma\psi,$$

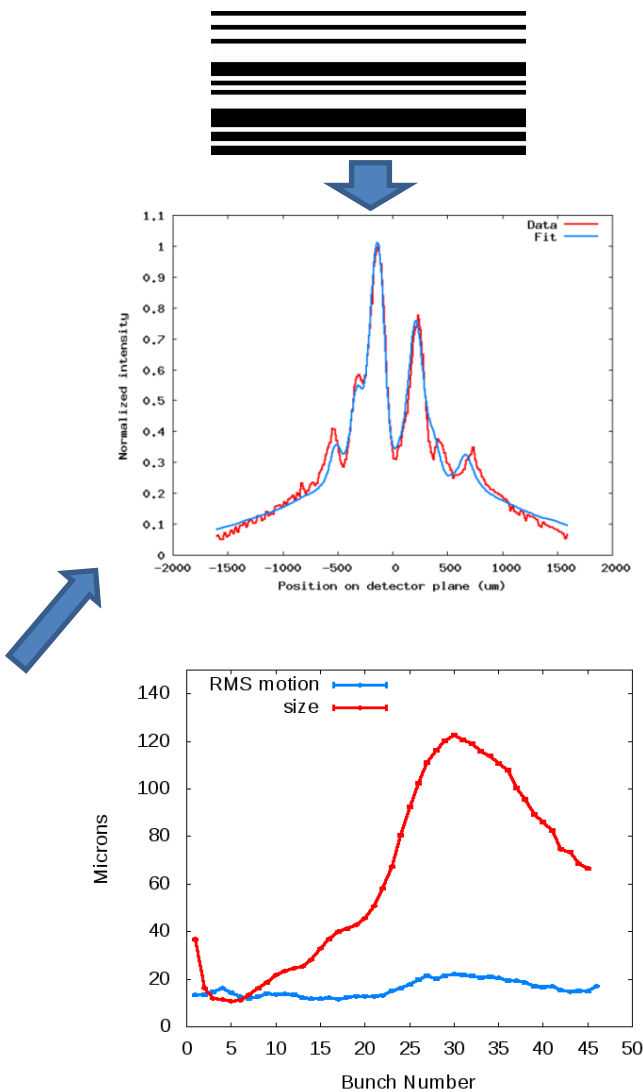
+

$$\eta = \frac{1}{2} \frac{\omega}{\omega_c} (1 + X^2)^{3/2},$$

Kirchhoff integral
over mask

(+ detector response)

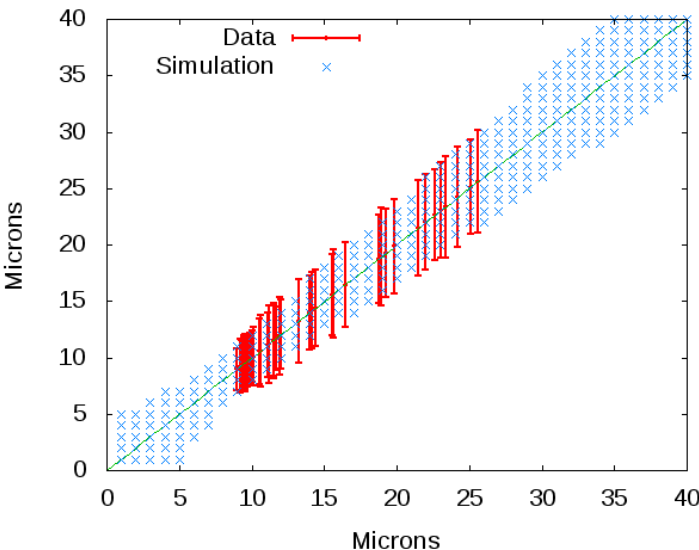
$$A_{\sigma,\pi}(y_d) = \frac{iA_{\sigma,\pi}(\text{source})}{\lambda} \int_{\text{mask}} \frac{t(y_m)}{r_1 r_2} e^{i\frac{2\pi}{\lambda}(r_1 + r_2)} \times \left(\frac{\cos \theta_1 + \cos \theta_2}{2} \right) dy_m,$$



Example of bunch-by-bunch data (electron-cloud blow-up study data). Single-shot data averaged for each bunch.

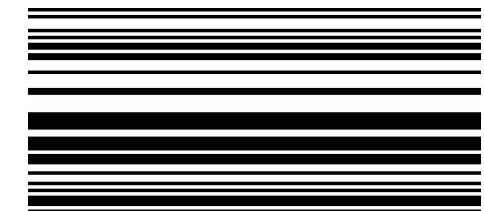
Hybrid: X-ray Coded Aperture

- Single-shot resolutions (statistics dominated) demonstrated of ~10 micron beams with single-shot resolutions of ~2 microns demonstrated at CesrTA.
- Expect to measure 4 micron beams (+/- 2 microns single-shot) at ATF2.
- Also plan to use at SuperKEKB.

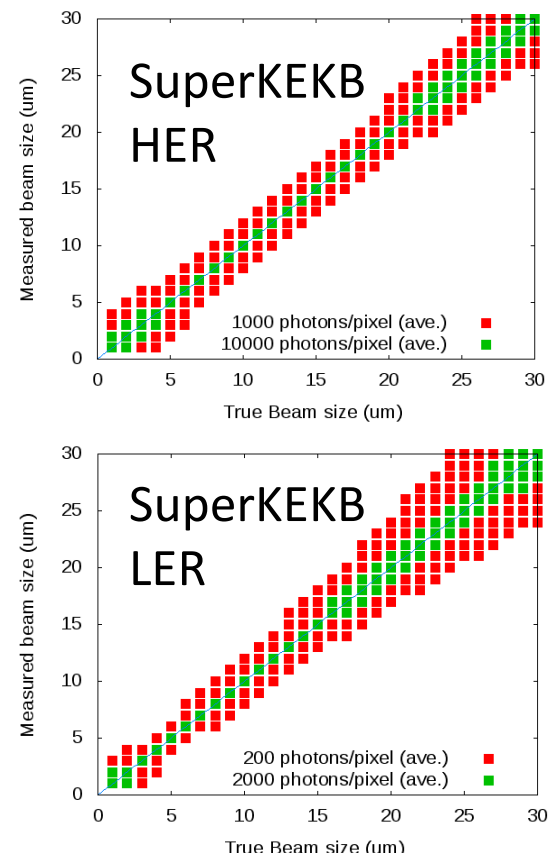


Single-shot resolution (simulation + measured spread at CesrTA)

- Red points: using 64-pixel detector of same type as at CesrTA
- Green points: using detector with improved photon detection efficiency at higher x-ray energies

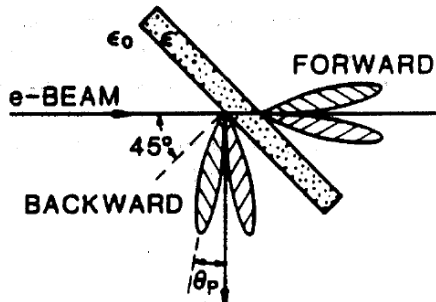


Uniformly Redundant Array (URA) for x-ray imaging to be used at SuperKEKB



OTR Monitor

- Optical Transition Radiation is radiation emitted when passes through boundary of two surfaces with different dielectric constants, such as vacuum and metal.
 - In backward direction, travels as if “reflected” from metal surface. In forward direction, travels along beam axis.

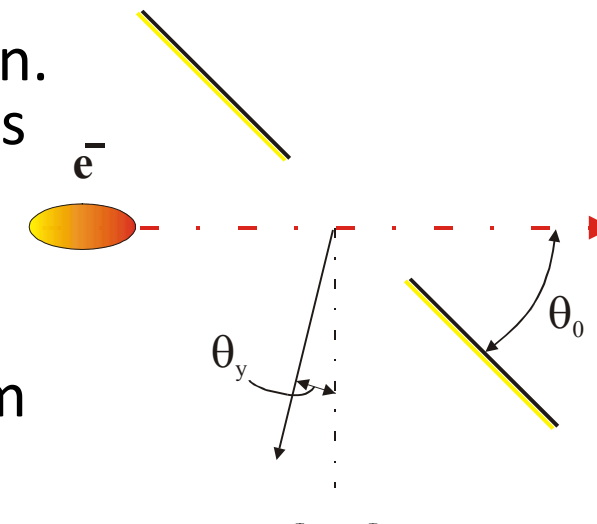


A.H. Lumpkin et al., NIM A296 151 (1990).
(via B. Gitter, CAA-TECH-NOTE-internal-#24)

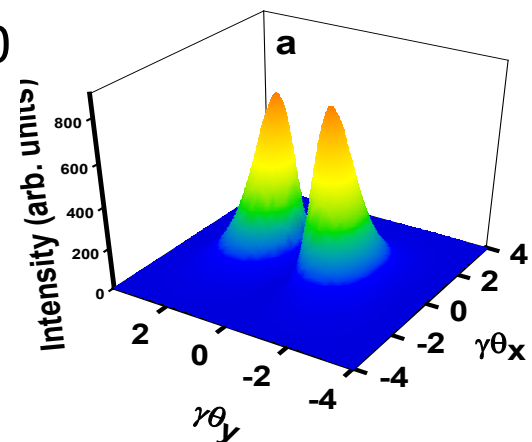
- Beam peaked like $1/\gamma$, like SR, the source can be much closer to the measurement aperture. (Don't have to be downstream of bend.)
- Beam can be imaged
 - Spatial resolution of 2 microns achieved in visible range (550 nm) using backward TR
[M. Ross, et al., SLAC Pub. 9280 \(2002\).](#)
 - Imaging in EUV (13.5 nm) proposed for submicron single-shot diagnostic.
[L.G. Sukhikh et al., NIM A 623 567-569 \(2010\).](#)
- Double-lobed structure of PSF may be used for visibility measurements similar to vertical polarization monitor.
 - Sub-micrometer resolution expected at ATF2
[A.Aryshev et al., Proc. IPAC10, MOPEA052 \(2010\).](#)
 - See A. Aryshev's talk (next!) for more!

ODR Monitor

- Beam goes through slit in conducting screen. Electric field on the electron beam polarizes the screen surface which emits radiation in the direction of specular reflection.
- Similar to OTR, but with hole in the middle, so non-destructive (as long as clear of beam tails).
- Produces an interference pattern similar to SR interferometer.
 - Proposed to be used as diagnostic by M. Castellano (M. Castellano, NIM A 394, 275 – 280 (1997))
- Vertical polarization component is sensitive to beam size.
- Tested at ATF extraction line.
 - Sensitivity to beam sizes down to 14 microns demonstrated.



ODR



ODR Monitor

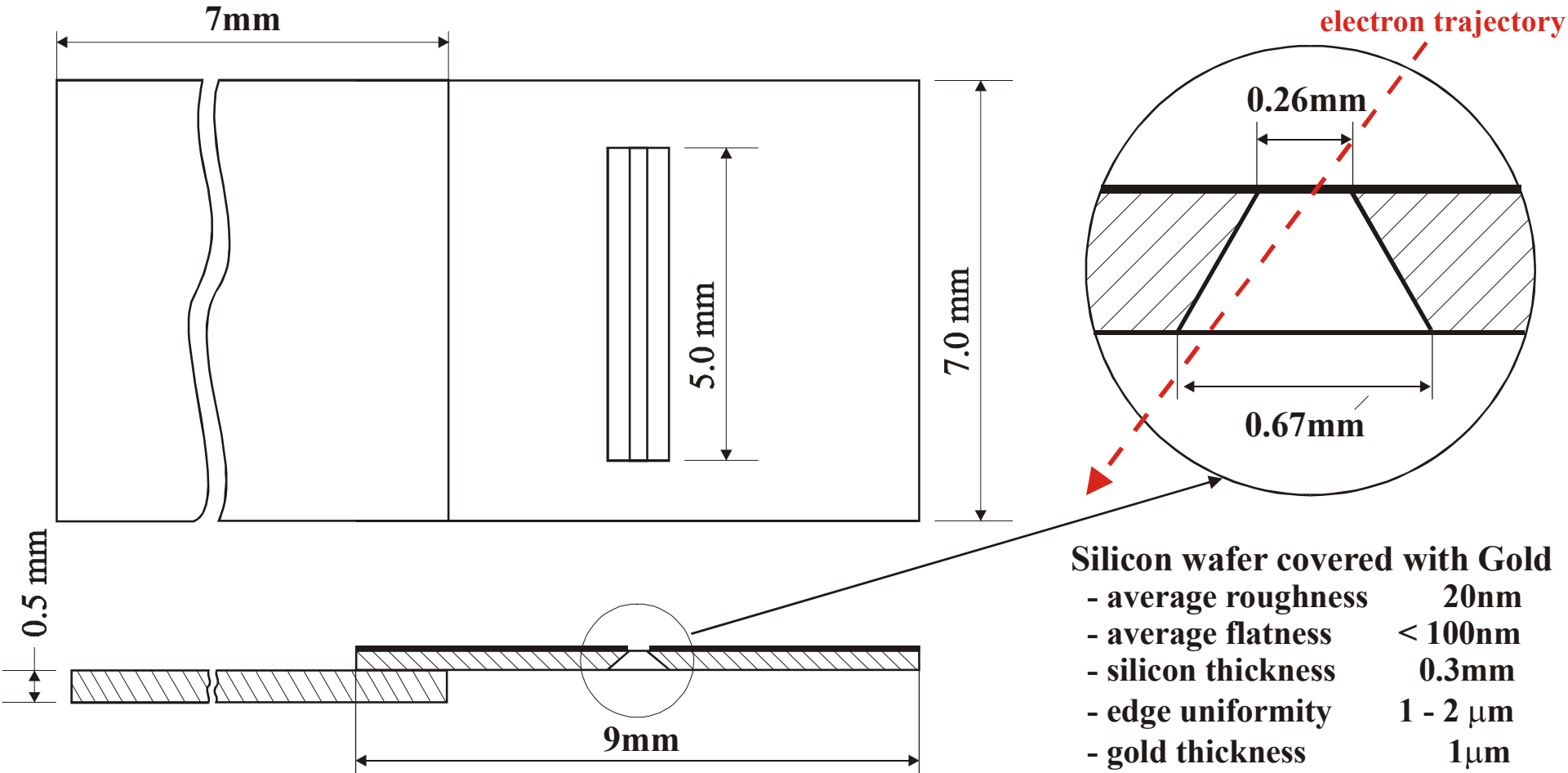
- Tests at CesarTA plan to push the wavelength frontier, with sub-micron resolution hoped for.
 - Visible (500 nm) -> UV (100 nm) -> x-ray
 - Shorter wavelength more sensitive to beam size, but produces fewer photons, so balance to optimize single-shot resolution.
 - Photon yield:
 - Slit half-width 320 μm at λ=500 nm
 - Optimal sensitivity:
 - Min. measurable beam size 16 μm at λ=500 nm
 - These numbers both scale down as λ does.
 - At 100 nm, slit half-width = 60 μm, beam size limit = 3 μm.
- Target slit will be placed in the CesarTA ring.

$$Z = \frac{\omega}{\omega_c} = \frac{2\pi a}{\gamma\lambda} < 1$$

$$\sigma > 0.05 \frac{\gamma\lambda}{2\pi}$$

ODR Monitor

A silicon wafer covered with a thin gold foil



| Silicon wafer covered with Gold | |
|---------------------------------|---------------|
| - average roughness | 20nm |
| - average flatness | < 100nm |
| - silicon thickness | 0.3mm |
| - edge uniformity | 1 - 2 μ m |
| - gold thickness | 1 μ m |

Laser Wire: Focused Waist

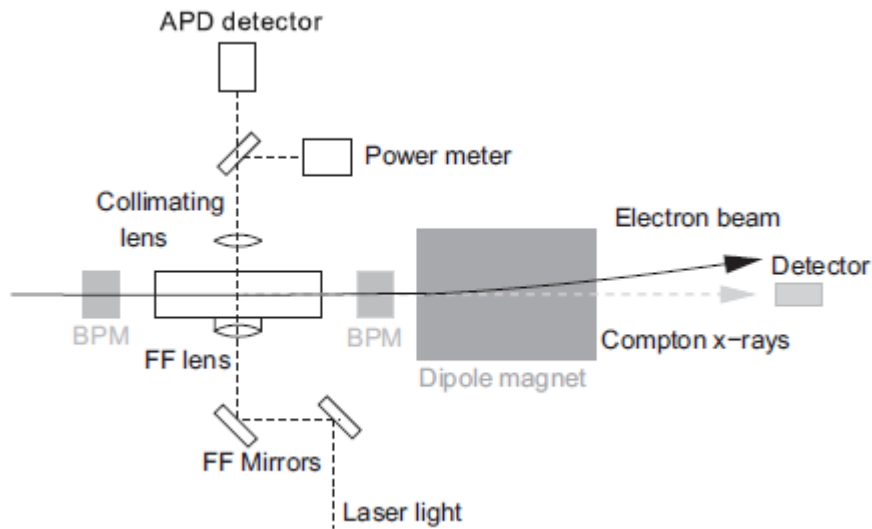
- Measures beam size by sweeping focused laser beam across bunch, and measuring inverse-Compton-scattering photons created.
- Resolution is determined by size of laser waist where beam intersects it:

$$\sigma_{measured} = \sqrt{\sigma_{laserwaist}^2 + \sigma_{beam}^2}$$

- Straightforward in principle, though a lot of work to make sure waist is properly focused, pulse-to-pulse variations are minimized and understood during scan, etc.

Laser Wire: Focused Waist

- Measurements at ATF extraction line managed a laser waist of 2.2 ± 0.2 microns, and measured beam sizes of 2.91 ± 0.15 microns.



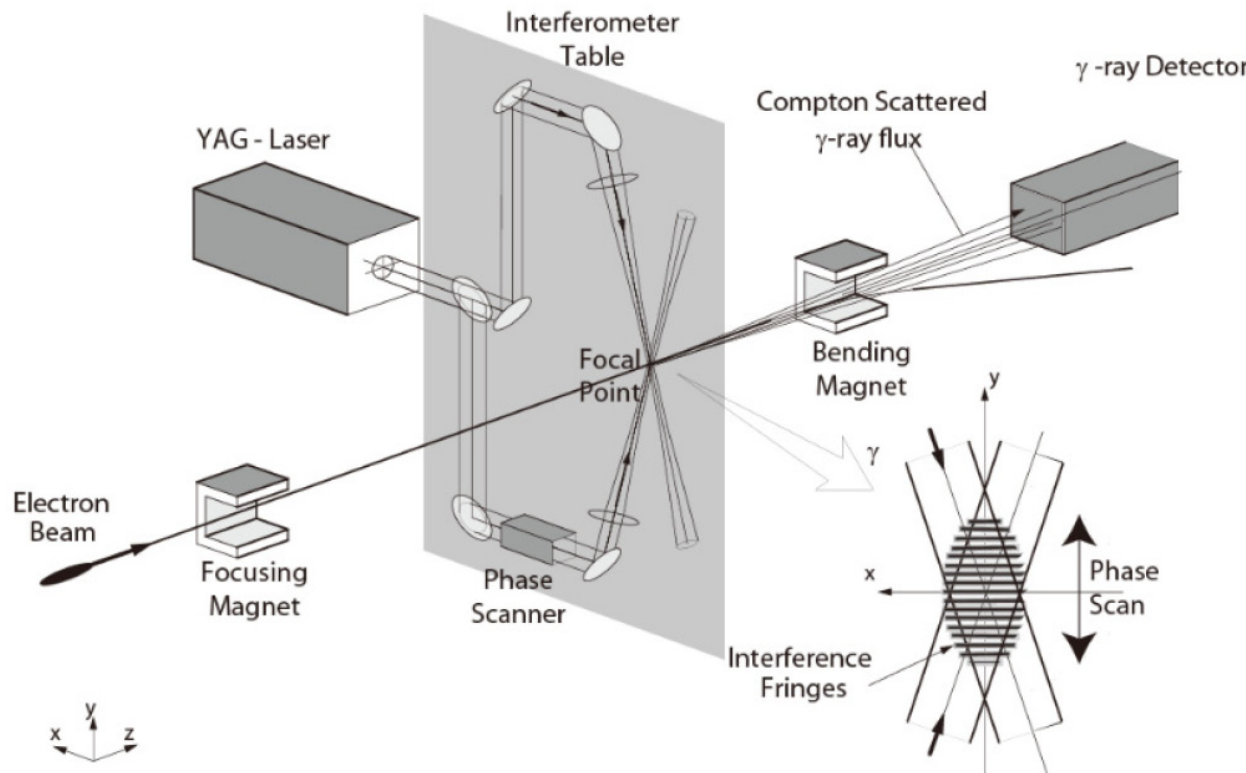
A. Aryshev et al. / Nuclear Instruments and Methods in Physics Research A 623 (2010) 564–566

- Measurements at ATF2 have gone down to 4.8 ± 0.3 microns.
 - Moving to new location in ATF2 to test with beam sizes below 1 micron (L.J. Nevay et al., IPAC11 TUPC158)

Laser Wire: Shintake Monitor

- Variant on laser wire: Instead of scanning a single focused beam, create an interference pattern between two laser beams in chamber, and pass electron beam between them.
- Bright fringes act like laser wires.
- Resolutions below 900 nm have been demonstrated, with a goal at the ATF2 of measuring 37 nm beam sizes.
- The highest resolution beam monitor out there at the moment.

Laser Wire: Shintake Monitor



- Beam size measured by modulation depth as phase of interference pattern is scanned across the beam.

$$\sigma_e = \frac{\lambda}{4\pi \sin(\theta/2)} \sqrt{2 \ln\left(\frac{|\cos \theta|}{M}\right)},$$

T. Shintake, Nucl. Instr. Meth. A311, 453 (1992).
T. Shintake et al., Proceedings of PAC95 (1995).

Laser Wire: Shintake Monitor

Setup at ATF2

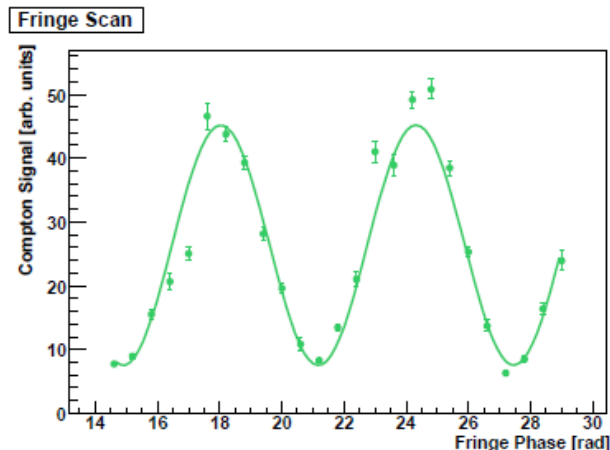
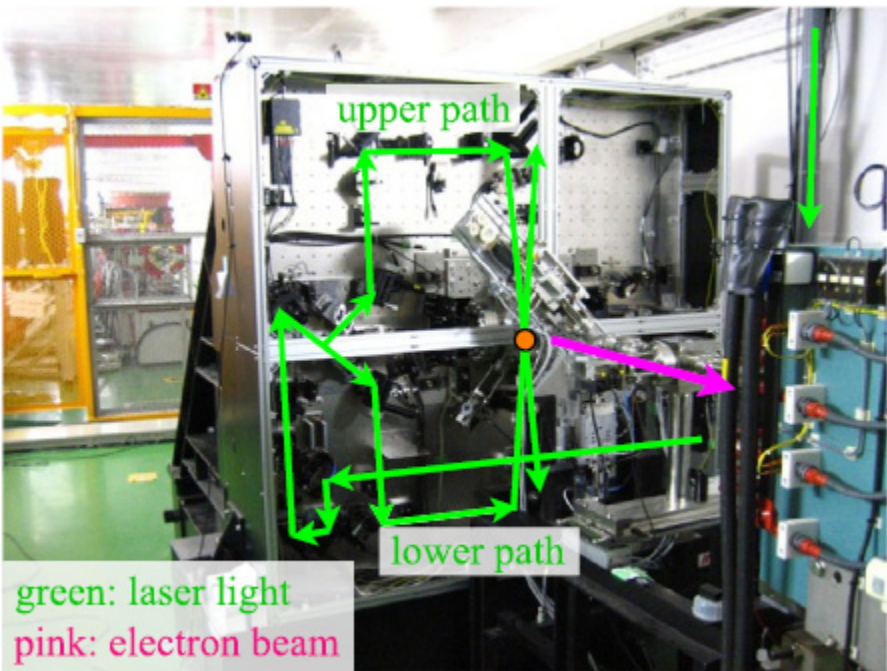
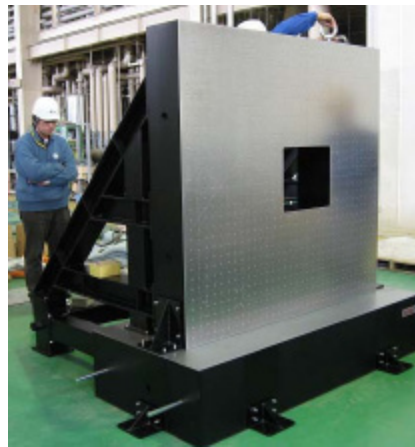


Figure 2: Beam size measurement

Y. Yamaguchi et al., Proc IPAC10, MOPE023 (2010).
Y. Kamiya et al., Proc IPAC10, MOPE022 (2010).
T. Kume et al., Proc IPAC10, TH4RFP084 (2010).

- So far demonstrated 860 ± 40 beam size measurement.



Laser Wire: Shintake Monitor

Setup at ATF2

- Technical challenges, limitations on resolution:
 - Vibration stabilization: nanometer order
 - Relative jitter between electron beam and interference pattern
 - Laser alignment accuracy
 - Maximize overlap and hence modulation depth
 - Laser temporal coherence
 - Phase spread
 - Phase jitter
 - Fringe tilt wrt beam vertical axis
 - Laser spherical wavefront
 - Curved interference pattern if focus off
 - Gamma background
- Taking above and other issues into consideration, expect 10% statistical and 6% systematic error for 1-minute measurement at 37 nm beam size.

Y. Yamaguchi et al., Proc IPAC10, MOPE023 (2010).

This will be an impressive achievement!

Large Angle Beamstrahlung Monitor

- Not strictly a pure beam size monitor:
 - Measures the *differences* in sizes, positions, etc. of two colliding beams.
 - Uses light generated as two bunches focus each other.
 - Similar to short-magnet SR
 - Also polarized like SR, with polarization pattern around edges of bunch depending on relative size, offset, etc. of partner bunch.
- Beamstrahlung first measured at SLS
- LABM tested at CesrTA
- Planned to install full set of diagnostics for both beams at SuperKEKB.
 - Test also planned at DAΦNE

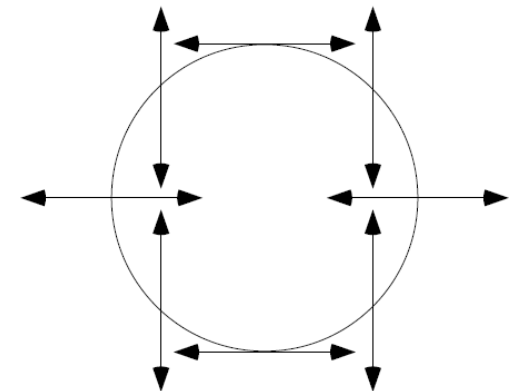
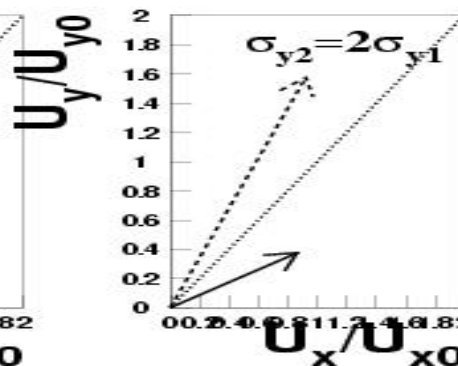
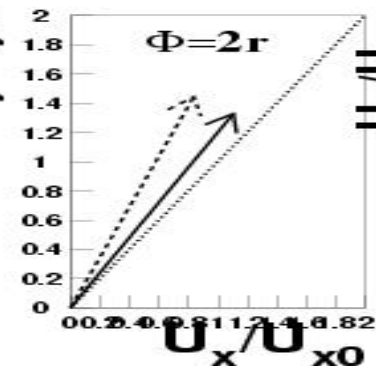
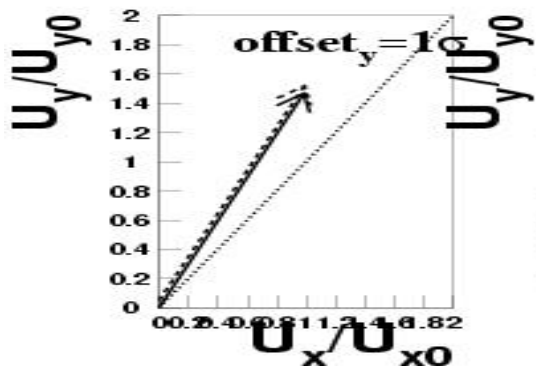
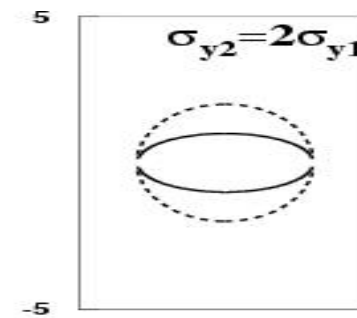
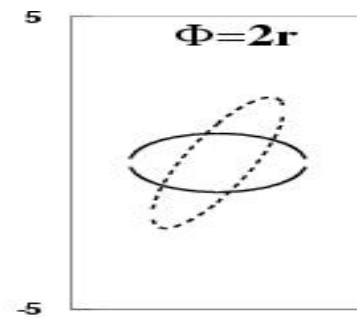
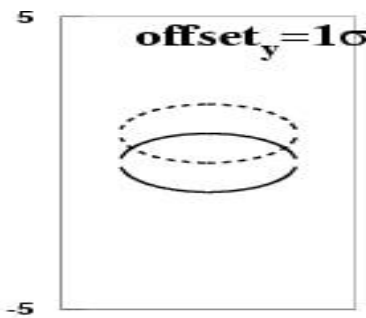


Figure 3: Eightfold polarization pattern for a particle bent in the horizontal direction.

G. Bonvicini

Large Angle Beamstrahlung Monitor

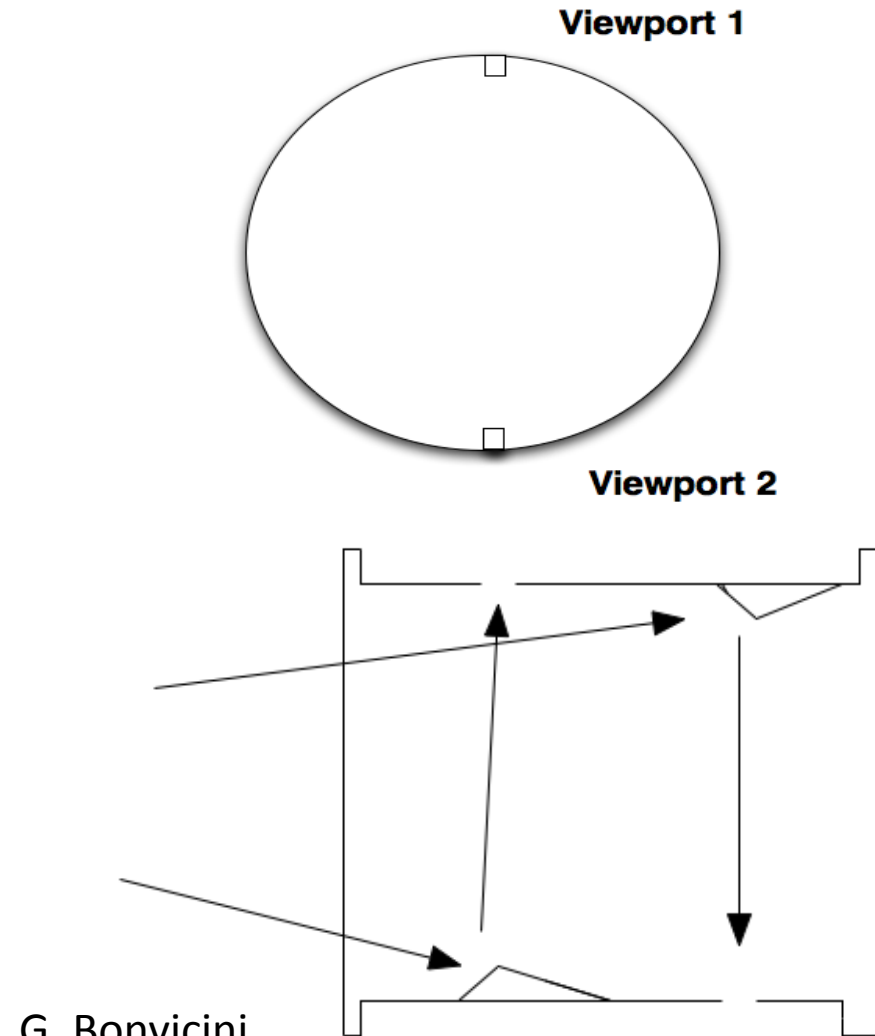
- The radiation of the particles of one beam due to the bending force of the EM field of the other beam
- Beamstrahlung POLARIZATION at specific azimuthal points provides unique information about the beam-beam geometry.



Large Angle Beamstrahlung Monitor

At SuperKEKB

- View port location at ± 90 degrees minimizes backgrounds, polarization measurement errors, and provides redundancy against beam orbit errors
- Located 4.8 m downstream of IP in HER, 3.7 m downstream in LER.
- Mirror and window sizes: 2.83X2 mm² and 2.1X2.1 mm²



Comments

- Single-shot versus integrating or scanning measurements:
 - Single-shot measurements may become more necessary for beam tuning, especially in colliders that push the margins of stability all the time, but not there exclusively, either.
 - Single-shot generally implies wide spectral acceptance (no monochromator).
 - Usually means a lot more work understanding the system. Simple analytical formulas don't work, lots of numerical crunching needed.
- Have not touched on detectors too much, but there will be a growing need to develop high-resolution, high-energy, and high-speed detectors.
 - High resolution: to minimize the amount of path length required for magnification
 - Available path length often limited.
 - High-energy, for detection efficiency at shorter wavelengths needed for better resolution.
 - High-speed, for single-shot measurements.

Possibilities for the Future

- Obvious extrapolations (some already being evaluated):
 - X-ray reflective (grazing incidence) optics
 - X-ray interferometer
 - Shorter wavelength Shintake Monitor?
 - Gamma-ray monitors?
- --Something else out there that we are completely missing?
- Let's think!